

RSC Advances



This is an *Accepted Manuscript*, which has been through the Royal Society of Chemistry peer review process and has been accepted for publication.

Accepted Manuscripts are published online shortly after acceptance, before technical editing, formatting and proof reading. Using this free service, authors can make their results available to the community, in citable form, before we publish the edited article. This *Accepted Manuscript* will be replaced by the edited, formatted and paginated article as soon as this is available.

You can find more information about *Accepted Manuscripts* in the [Information for Authors](#).

Please note that technical editing may introduce minor changes to the text and/or graphics, which may alter content. The journal's standard [Terms & Conditions](#) and the [Ethical guidelines](#) still apply. In no event shall the Royal Society of Chemistry be held responsible for any errors or omissions in this *Accepted Manuscript* or any consequences arising from the use of any information it contains.

1 Real-time Monitoring of the Drying of Extruded Granules in a Fluid-bed Dryer Using
2 Audible Acoustic Emission Chemometrics

3

4 Hisayoshi Aoki,⁺ Yusuke Hattori,⁺ Makoto Otsuka^{*}

5

6 *Research Institute of Pharmaceutical Sciences, Faculty of Pharmacy,*

7 *Musashino University, 1-1-20 Shinmachi Nishitokyo-shi, Tokyo 202-8585, Japan*

8 ⁺, These authors contributed equally to this work.

9

10

11

12

13

14

15

16

17

18

19 ^{*}Corresponding author. Tel. and fax: +81-42-468-8658

20 E-mail address: motsuka@musashino-u.ac.jp (M. Otsuka)

21

22

23 **Abstract**

24 The purpose of this study was an attempt to adapt the audible acoustic emission (AAE)
25 sound measurement method for the on-line monitoring of the fluid-bed drying progress of
26 pharmaceutical granules. The granules were prepared by extrusion-granulation based on a
27 formulation of 6.7:2:1 lactose/starch/crystalline cellulose. After the granulation process, the
28 drying process was performed in a fluid-bed dryer at 27 or 42°C, and AAE sound was
29 measured using a digital voice recorder. The recorded signals were transformed into
30 frequency spectra by using fast Fourier-transformation function. Samples were collected
31 every 60 seconds to determine the moisture content of the granules. The calibration models
32 to predict the moisture content of the granules were constructed based on AAE frequency
33 spectra by using the partial least squares regression method after area normalized function. In
34 order to test the robustness of the calibration model obtained under different dry operating
35 conditions (air temperature) with various acoustic environments (noise), the moisture content
36 of the granules was predicted based on AAE frequency spectra containing noise. The
37 external validation results suggested that the calibration model could be applied to any data
38 set. The regression vector indicated that the sound in the low-frequency range might have
39 been caused by the contact of the granules upon over-hydration at the initial stage of the
40 drying process. In contrast, the sound at high frequencies might have been caused by friction
41 of the dried granules later in the drying process.

42

43 **Keywords:** process analytical technology; robustness of the calibration model; fluid-bed
44 drying; adapt audible acoustic emission sound; partial least squares regression; drying
45 process of granules
46
47

48 **Introduction**

49 Since granules have several advantages as a pharmaceutical dosage form compared with
50 powder, such as, better flowability, wettability, mixing uniformity, easy control of their dust,
51 and good compressibility, granules are prepared to agglomerate powdered materials into
52 larger sizes by using various kinds of granulator. The properties of the final granular
53 products are affected by operating conditions during the drying process and the kind of
54 granulator. The drying process of agglomerates of powdered materials is, therefore, a crucial
55 operation to make high-quality granular dosage forms in the pharmaceutical industry. These
56 are important properties in order to achieve fast, gentle and uniform particle drying. Owing
57 to the high drying rate, associated high quality, and economic benefits, fluid-bed drying has
58 been proposed as the method of choice over to other drying techniques.

59 In recent years, in order to improve the quality of pharmaceutical products, regulatory
60 authorities such as the US Food and Drug Administration and the International Conference
61 on Harmonization have proposed Process Analytical Technology (PAT) initiative forms
62 based on the pharmaceutical Good Manufacturing Practice rules for the 21st century.^{1, 2} They
63 requested real-time control of drug product quality and the application of Quality by Design
64 principles to monitor and control manufacturing processes using PAT tools.³⁻⁵

65 To control the drying process, conventional chemical (Karl Fischer titration) and physical
66 (heat balance) methods are used routinely for the determination of water content in
67 pharmaceutical products. However, they are hard to perform as real-time monitoring of the
68 drying because both methods are time-consuming and costly. Recently, near-infrared (NIR)
69 spectroscopy has been introduced in the pharmaceutical industry because it is

70 non-destructive and requires no or minimal sample preparation and provides immediate
71 delivery of results. In particular, in combination with chemometrics, NIR spectroscopy
72 provides an ideal method of extracting quantitative information from multi-component
73 chemical samples in the pharmaceutical field. The most widely used chemometric methods
74 include multiple linear regression, principal component analysis/principal component
75 regression, and partial least squares (PLS) regression.⁶ For example, chemometric NIR
76 spectroscopy has been used to determine active pharmaceutical ingredients off-line and
77 on-line, tablet excipient content,⁷⁻¹⁰ drug stability,¹¹ particle size of powders,¹² tablet
78 mechanical strength,^{13, 14} and dissolution rate.¹⁴⁻¹⁷ However, it is costly to establish many
79 NIR spectroscopy instruments on production lines in factories.

80 On the other hand, mechanical sound during chemical and/or pharmaceutical processes is
81 useful information for evaluating the degree of product completion for veteran technicians in
82 industry. On the basis of veteran technical experts' knowledge and skill for controlling
83 manufacturing processes, acoustic emission (AE) technology was developed for process
84 monitoring. AE monitoring has the advantage of being a real-time, noninvasive technique,
85 the same as NIR spectroscopy. AE and NIR methods capture the mechanical and optical
86 signatures of events taking place during processing, respectively.³ However, the NIR method
87 requires installation of a micro-fiber probe and a line into the sample powder for measuring,
88 but the AE method does not need a direct line-of-sight to the material of interest and
89 therefore requires no alteration of manufacturing equipment.

90 To take advantage of the ease of installation of measurement devices and good
91 measurement accuracy, the AE analysis method was developed in chemical and

92 pharmaceutical fields as a PAT pilot study, and **there are several reports on AE**
93 **application studies.**¹⁹⁻²⁹ The research can be divided into two types; with ultrasonic (greater
94 than 20,000 Hz) and audible (approximately 20–20,000 Hz) AE sensors.

95 Ultrasonic AE sensors can be easily attached to the container wall of pharmaceutical
96 machines to detect sounds. For example, the effects of operation conditions on the acoustic
97 signal during tablet compression,¹⁸ the roller compaction^{19, 20} and table coating processes,²¹
98 mixing process,²² particle measurement,^{23, 24} and agitating granulation²⁵ have been studied.
99 In contrast, audible AEs differ from ultrasonic AEs in terms of the setting of measurement
100 devices, because they propagate through air with minimal attenuation²⁶⁻²⁹ and therefore
101 equipment contact is not required for detection. Microphones suspended at the top of
102 granulator air exhausts were also shown to be sensitive to granulation-based pharmaceutical
103 formulation for identifying the granulation end-point.^{26, 28}

104 On the other hand, one of the emerging on-line non-invasive PAT approaches for process
105 characterization is acoustic chemometrics, since interpretations of these complex AE data are
106 most effectively performed through the use of modern chemometric methods.^{30, 31} On-line
107 process monitoring of the fluid-bed drying process was investigated by using acoustic
108 chemometrics.^{32, 33} Ihunegbo et al.³⁴ investigated the feasibility of quantitative on-line
109 monitoring of the drying progress and end-point determination of pharmaceuticals dried in a
110 heated fluid-bed based on audible and ultrasonic AEs by chemometrics. They concluded that
111 the final prediction results were satisfactory for monitoring of the drying progress and
112 end-point determination by the PLS method. However, they did not report scientific evidence

113 of the calibration models to predict individual pharmaceutical properties of the final
114 products.

115 The present study is an attempt to adapt the audible acoustic emission sound measurement
116 method for the on-line monitoring of the fluid-bed drying progress of pharmaceutical
117 granules, and to clarify the scientific background of the calibration model to predict moisture
118 content in granules by audible acoustic emission (AAE) frequency spectrum/chemometric
119 analysis.

120

121 **Materials and methods**

122 *Materials*

123 Lactose monohydrate (Pharmatose® 200M) from DMV (Veghel, The Netherlands), potato
124 starch from Kosakai Pharmaceutical Co., Ltd. (Japan), microcrystalline cellulose
125 (CEOLUS® PH-102) from Asahi Kasei Co., Ltd. (Tokyo, Japan), and hydroxypropyl
126 cellulose (HPC-L®) from Nippon Soda Co., Ltd. (Tokyo, Japan) were used. The lactose
127 served as a filler, potato starch as a disintegrating agent, microcrystalline cellulose as a
128 segregation preventive agent, and HPC-L as a binding agent. Granules comprising mainly
129 lactose, potato starch, microcrystalline cellulose, and HPC-L were prepared. This
130 formulation was based on a standard 6.7:2:1 lactose/starch/microcrystalline cellulose
131 mixture.

132

133 *Preparation of granules*

134 A total of 200.0 g of lactose, 60.0 g of potato starch, 30.0 g of microcrystalline
135 cellulose, and 10.0 g of HPC-L, were mixed in a polyethylene bag for 3 minutes by
136 hand. Purified water was added and the mixed was then kneaded in a mortar and pestle.
137 Granules, 1 mm in diameter, were prepared by extrusion granulation (KAR-130, Tsutsui
138 Scientific Instruments Co., Ltd., Tokyo, Japan). After the granulation process, drying was
139 performed in a fluid-bed dryer with a chamber made of glass (SP-15, 160 mm in diameter
140 and 6.0 L in volume, Okada Seiko Co., Ltd., Tokyo, Japan), as shown in Figure 1. A
141 sampling port was located 3 cm from the bottom of a chamber of the dryer, and granular
142 samples was withdrawn using a plastic sampling bar with a diameter of 15 mm. Fluid-bed
143 dryer operation conditions were fixed during all processes as follows: warming up time was
144 15 min at 42°C and rotor speed was 180 rpm. The granulation experiments were repeated
145 three times in each group. Outlet air temperature was measured using a temperature sensor,
146 and the temperature of outlet air was set at 42°C for the groups 1, 2 and 8, and at 27°C for
147 group 3. Group 2 involved drying under conditions (outlet air was set at 42°C) with noise
148 (**Japanese pop music, a vacuum cleaner, or a tableting machine**) to test the robustness for
149 the audible acoustic emission calibration model. A portable stereo radio CD player, a
150 vacuum cleaner, and a tableting machine were placed at a distance of 30 cm from the dryer
151 as sources of noise, respectively.

152

153 Figure 1

154

155 *Measurement of moisture content*

156 **The samples of approximately 3g were collected every 60 seconds 16 times using the**
157 **sampling bar during the drying process, and then the collected samples were weighed**
158 **accurately by an electronic analytical balance.** To determine the moisture content of the
159 granules, drying loss at 70°C for 24 hours was estimated. To evaluate the variability among
160 batches, the procedures were repeated multiple times and the moisture contents of the
161 granular samples were recorded. All batches were evaluated for the time required to reach a
162 point when there was no change in mass of the samples over time as the drying had finished.

163

164 *Acoustic signal measurements*

165 The acoustic sensor used was a digital voice recorder (RR-XS350, Panasonic Co., Ltd.,
166 Tokyo, Japan). The recorder was placed at a distance of 0.5 cm from the wall of the lowest
167 portion of the chamber of the fluid-bed dryer. Audible acoustic emission signals were
168 recorded as a waveform at a sampling rate of 44.1 kHz during the drying process. The
169 recorded AAE signals were transformed into frequency spectra every 60 seconds by using
170 the fast Fourier transformation function of Audacity® (Audacity 2.0.5,
171 <http://audacity.sourceforge.net>) as the calibration data. The AAE frequency spectra for the
172 semi-external validation data were transformed from raw signals of the groups 1, 2 and 3 at
173 every 61 seconds, respectively. In contrast, the spectra for the external validation data were
174 transformed from raw signals of the group 8 at every 60 seconds.

175

176 The FT-AAE frequency spectra were calculated at intervals of 1 second and window size
177 of 4096 by using Blackman-Harris window transformation in the frequency range between

178 0.01 and 22 kHz. The frequency spectra were converted from amplitude into sound pressure
179 level L_P according to the following expression.³⁵

$$180 \quad L_P = 10 \log_{10} \frac{P^2}{P_0^2} \quad (1)$$

181 where P is the actual sound pressure and P_0 is the reference sound pressure which is 20 μPa
182 in air. The actual sound pressure has a relationship with the electromotive force E described
183 in the following equation,

$$184 \quad E = S + 10 \log_{10} P^2 \quad (2)$$

$$185 \quad P = 10^{\frac{E-S}{20}} \quad (3)$$

186 where S is sensitivity of the microphone. Substituting Eq. (3) to Eq. (1), the following
187 equation can be derived,

$$188 \quad L_P = E - S + 94 \quad (4)$$

189

190

191 *Partial least squares regression*

192 A chemometric analysis was performed using the partial least squares (PLS) regression
193 method associated with the Pirouette software ver. 4.5 (Infometrix Corporation, Woodinville,
194 U.S.A.). The moisture contents (the dependent variable) of the granules were estimated
195 based on a total of 144 spectra (independent variables) involving groups 1, 2, and 3 by PLS.
196 The PLS calibration models were constructed by cross-validation using the leave-one-out
197 (LOOCV) method. The optimum number of factors was taken to be that leading to a

198 minimum value in the prediction residual error sum of squares (PRESS) versus PLS
 199 component graph, the former being defined as:

$$200 \quad PRESS = \sum_{i=1}^n (\hat{y}_i - y_i)^2 \quad (5)$$

201 where \hat{y}_i and y_i correspond to the moisture level of each granular sample predicted by the AE
 202 method and the reference method, respectively. The goodness of calibration and prediction
 203 was assessed in terms of the root mean square error (RMSE):

$$204 \quad RMSE(\%) = \sqrt{\frac{\sum_{i=1}^n (\hat{y}_i - y_i)^2}{n}} \quad (6)$$

205 which was termed RESEC for calibration and RMSEP for prediction.

206

207

208 **Results and discussion**

209 *Frequency spectra of granules during the drying process*

210 Figure 2 shows a typical example of an AAE waveform of audible acoustic sound during
 211 the drying process of extruded granules in the fluid-bed dryer. The AAE waveforms were
 212 transformed into AAE frequency spectra using the Fourier-transformation function.

213 **Figure 3 (a)** shows change of raw frequency spectra of AAE sound during the drying
 214 process of extruded granules in the fluid-bed dryer. The sound pressure level below 0.1 kHz
 215 significantly decreased with increasing of the time, but that above 1 kHz increased with a lot
 216 of noise. It was considered that there were a number of noises in the high-frequency range,
 217 which made it difficult to analyze the frequency spectrum.

218 To clarify time-dependent changes in the frequency spectra of granular samples during the
219 drying process, the raw spectra were converted to area normalized frequency spectra. **Figure**
220 **3 (b)** shows change of the area normalized frequency spectra of AAE sound during the
221 drying process of extruded granules in the fluid-bed dryer. In the area normalized frequency
222 spectra, sound pressure level at lower than 1 kHz significantly decreased with increasing
223 time, but that above 1 kHz was almost constant.

224

225 **Figures 2 and 3**

226

227 *Construction of partial least squares model*

228 To predict the moisture content of granules, the calibration models were constructed based
229 on frequency spectra by using the PLS method after area normalized function. **Figure 4 (a)**
230 shows the correlation between the actual and predicted moisture contents of group 1
231 (standard drying conditions) obtained by the PLS method, and their chemometric parameters
232 are summarized in Table 1. The relationship between the actual and predicted moisture
233 contents shows a straight line with a slope of 0.992, y-intercept of 0.0595, and correlation
234 coefficient of 0.992. The PRESS and the RMSECV were evaluated to be 31.5 and 2.18 by
235 the leave-one-out method in the PLS method, and the other parameters also supported the
236 assertion that the obtained calibration model involving the first 4 latent variables (LV) could
237 predict the moisture content in the granular samples with sufficient accuracy.

238

239 **Figure 4 (a) and Table 1**

240

241 *Effects of acoustic environment and drying operation conditions on the robustness of the*
242 *calibration model*

243 In order to test the robustness of the calibration model obtained under dry operating
244 conditions of the various acoustic environments, the moisture contents of the granules were
245 predicted based on acoustic frequency spectra containing noise. Group 2 was dried under
246 experimental conditions involving the following type of noise. The drying experiments for
247 the granules were performed with Japanese pop song were played on a portable radio CD
248 player, a vacuum cleaner, and a tableting machine. As shown in Table 1, the chemometric
249 parameters for group 2 supported the assertion that the calibration model involving the first 4
250 LVs could be predicted sufficient accurate the moisture content in the granular samples with
251 sufficient accuracy. Those for group 4, involving both group 1 and group 2, also indicated
252 that the model involving the first 5 LVs could provide accurate predictions. The results
253 suggested that the calibration model was not affected by the typical noise in the measurement
254 environment, and the moisture content of the granules could be predicted based on AAE
255 frequency spectra containing noise.

256 It is well known that the drying process is dependent on change of the outer air
257 temperature, so the effect of outlet air temperature on the drying process was investigated.
258 Group 3 was dried under lower-temperature conditions at 27°C, and the chemometric
259 parameters indicated that the calibration model involving the first 4 LVs could predict the
260 moisture content with sufficient accuracy, as shown in Table 1. Those for group 5, involving

261 temperature variations (27 and 42°C), also indicated that the model involving the first 5 LVs
262 could provide accurate predictions.

263 Finally, the drying process in a fluid-bed dryer is affected by various process operating
264 conditions, such as outer air temperature, humidity, and noise. Therefore, the combined
265 effects of drying temperature variations and environmental noise on the robustness of the
266 calibration model were investigated. Groups 6 and 7 underwent drying conditions involving
267 both temperature variations and environmental noise. **Figure 4 (b)** shows the relationship
268 between the predicted and actual moisture contents for group 7, with a straight line with a
269 slope of 0.984, y-intercept of 0.168, and correlation coefficient constant of 0.984. The
270 calibration model for group 7 consisted of the first 5 LVs involving 72.6% cumulative
271 variance, and the parameters indicated that the model could predict the moisture content with
272 sufficient accuracy, as shown in Table 1.

273

274 **Figure 4 (b)**

275

276 *Validation of the fitted calibration models based on external validation data*

277 For validation of the PLS calibration models to predict the moisture content of the
278 granules, the other frequency spectra as an external validation data set were applied to the
279 obtained calibration models. **Figure 4 (c)** and Table 2 show the suitability of each
280 calibration model of the semi-external validation data for groups 1-3 and external validation
281 data for group 8. The semi-external validation data of G1, G2, and G3 were evaluated using
282 all calibration models, and then the best R^2 s were obtained by using the calibration models

283 that were created using the individual data sampling time at every 61 seconds. However,
284 there was no model that could be applied to the other data sets, except for the model based
285 on group 7. The R^2 for groups 1, 2, and 3 were 0.985, 0.994, and 0.928 by using the
286 calibration model for group 7, respectively. These results suggest that the calibration model
287 based on group 7 could be applied to any group data set.

288

289 **Figure 4 (c) and Table 2**

290

291 *Scientific background of the PLS calibration model to predict the moisture content in the*
292 *granules based on the AAE frequency spectrum*

293 PLS regression is effective in the extraction of features and regularity, and modeling of
294 unstable, large, and complex numerical data. However, the disadvantages of PLS regression
295 are the difficulty of interpretation of the factors, and it is also necessary to determine the
296 number of factors to be used. Therefore, in order to provide the scientific evidence of the
297 ability of the PLS models based on AAE frequency spectra to predict the moisture content of
298 the granules, relationships between the loading or regression vector and information on the
299 formulation powder during drying were examined.

300 **Figure 5** shows the loading vectors for first and second LVs of the calibration model to
301 predict moisture content in the granules. The loading vectors for the first and second LV
302 contained 58.6% and 7.5% of the total variance, respectively. The loading vector for the
303 first LV had the positive broad peaks at 10-100 Hz and positive specific peaks at 484 and
304 1216 Hz. It had negative peaks at 656, 1442, and 15,000-22,000 Hz. The vector for the

305 second LV had positive broad peaks at 86, 204, and 355 Hz and negative peaks at 667,
306 947-1141, and 2000-3500 Hz. The result of the first loading vector indicates that the sound
307 with lower frequency than 100 Hz was converted into sound higher than 15,000 Hz. The
308 vector for the second LV was due to mid-frequency range sound transformation, which
309 means that sound of 60-200 Hz was converted into sound of 1000-4000 Hz.

310 **Figure 6** shows the relationship between the scores of first LV and second LV for the
311 calibration model based on group 7 to predict the moisture content in the granules. In the
312 first half of the drying process, the first LV decreased, in the second half, it gradually
313 reached a constant value of -2. In contrast, the second LV increased in the first half and
314 decreased in the second half.

315 **Figure 7** shows the regression vector plot as a weighting function of the calibration model
316 for group 7, involving temperature variations and environmental noise. In the regression
317 vector, positive peaks were observed at a relatively low-frequency range at 100 Hz, 200 Hz,
318 340 Hz, 840 Hz, and 1570 Hz. In contrast, the negative peaks were observed at a higher
319 range at around 2030 Hz and 3440 Hz. These results indicated that the peaks at lower
320 frequency decreased during the drying process, but the peaks at higher frequency increased.
321 The sound in the low frequency range might have been caused by the contact of the granules
322 upon over-hydration at the initial stage of the drying process. In contrast, the sound at high
323 frequencies might have been caused by friction of the dried granules later in the drying
324 process.

325

326 **Figures 5, 6, and 7**

327

328 *Kinetic evaluation of fluid-bed drying process of the extruded granules.*

329 **Figure 8** shows the changes of the moisture contents in the granules for groups 1, 2, and 3
330 predicted by using the best-fitted PLS model. Predicted moisture content profiles were
331 generally consistent with measured values. It is well known that there are three phases (i.e.
332 pre-heating period, constant drying rate period, and falling drying rate period) during the
333 drying process, as reported previously.³⁶ The pre-heating period is the time required to reach
334 a certain dynamic equilibrium temperature determined by the drying conditions of the initial
335 temperature. The constant drying rate period is a period during which the cooling rate due to
336 evaporation of free water is equal to heating by hot air, and the drying rate is constant. In
337 other words, as long as free water is present on the granule surface, the constant rate drying
338 period continues. The falling drying rate period is the time required to dry the water present
339 inside the granules. As shown by the results for various drying conditions, the drying process
340 of the granules could be separated into pre-heating period, constant drying rate period, and
341 falling drying rate period by the AAE chemometrics. The drying process of the granules
342 could also be divided into two processes; the former process might be due to the sound
343 caused by the collision of wetted granules, and the latter process might be the sound caused
344 by friction of dried granules.

345

346 **Figure 8**

347

348 **Conclusion**

349 The present study demonstrated the usefulness of real-time monitoring using AAE
350 analysis to predict the moisture content of granules and product quality parameters during the
351 fluid-bed drying process in real time. To determine the parameters, a PLS model based on
352 AAE frequency spectra and loss on drying measurements was constructed under different
353 dry operating conditions with various acoustic environments. This technique facilitated the
354 construction of a robust model with no variability from batch to batch. This technique
355 provides for better understanding and control of the drying process in a less expensive
356 manner.

357

358 **Acknowledgments**

359 This research was supported in part by a Grant for Musashino-Jyoshi Gakuin.

360

361

362

363 **References**

- 364 1 Process Analytical Technology (PAT) Initiative, U.S. Food and Drug Administration
365 Center for Drug Evaluation and Research Home Page,
366 <http://www.fda.gov/AboutFDA/CentersOffices/OfficeofMedicalProductsandTobacco/CDER/ucm088828.htm>, (accessed August 2009).
- 368 2 International Conference on Harmonization of Technical Requirements for Registration
369 of Pharmaceuticals for Human Use. Pharmaceutical Development Q8 (R2),
370 <http://www.fda.gov/downloads/Drugs/GuidanceComplianceRegulatoryinformation/Guidances/ucm073507.pdf>, (accessed August 2009).
- 372 3 S. Matero, F. V. Den Berg, S. Poutiainen, J. Rantanen, J. Pajander, Towards Better
373 Process Understanding: Chemometrics and Multivariate Measurements in
374 Manufacturing of Solid Dosage Forms, *J. Pharm. Sci.*, 2013, **102**(5), 1385-1403.
- 375 4 L. X. Yu, Pharmaceutical Quality by Design: Product and Process Development,
376 Understanding, and Control, *Pharm. Res.*, 2008, **25**(10), 781-791.
- 377 5 T. De Beer, A. Burggraeve, M. Fonteyne, L. Saerens, J. P. Remon, C. Vervaet, Near
378 infrared and Raman spectroscopy for the in-process monitoring of pharmaceutical
379 production processes, *Int. J. Pharm.*, 2011, **417**(1-2), 32-47.
- 380 6 H. Martens, T. Naes, *Multivariate calibration*, 1989, New York: John Wiley & Sons.
- 381 7 M. Blanco, A. Eustaquio, J. M. González, D. Serrano, Identification and quantitation
382 assays for intact tablets of two related pharmaceutical preparations by reflectance

- 383 near-infrared spectroscopy: validation of the procedure, *J. Pharm. Biomed. Anal.*, 2000,
384 **22**(1), 139-48.
- 385 8 L. Alvarenga, D. Ferreira, D. Altekruze, J. C. Menezes, D. Lochmann, Tablet
386 identification using near-infrared spectroscopy (NIRS) for pharmaceutical quality
387 control, *J. Pharm. Biomed. Anal.*, 2008, **48**(1), 62-69.
- 388 9 C. Bodson, E. Rozet, E. Ziemons, B. Evrard, P. Hubert, L. Delattre, Validation of
389 manufacturing process of Diltiazem HCl tablets by NIR spectrophotometry (NIRS), *J.*
390 *Pharm. Biomed. Anal.*, 2007, **45**(2), 356-361.
- 391 10 A. S. Zidan, M. J. Habib, M. A. Khan, Process Analytical Technology: Nondestructive
392 Evaluation of Cyclosporine A and Phospholipid Solid Dispersions by Near Infrared
393 Spectroscopy and Imaging, *J. Pharm. Sci.*, 2008, **97**(8), 3388-3399.
- 394 11 J. K. Drennen, R. A. Lodder, Nondestructive near-infrared analysis of intact tablets for
395 determination of degradation products, *J. Pharm. Sci.*, 1990, **79**(7), 622-627.
- 396 12 P. Frake, I. Gill, C. N. Luscombe, D. R. Rudd, J. Waterhouse, U. A. Jayasooriya,
397 Near-infrared mass median particle size determination of lactose monohydrate,
398 evaluating several chemometric approaches, *Analyst.*, 1998, **123**(10), 2043-2046.
- 399 13 M. Otsuka, I. Yamane, Prediction of Tablet Hardness Based on Near Infrared Spectra of
400 Raw Mixed Powders by Chemometrics, *J. Pharm. Sci.*, 2006, **95**(7), 1425-1433.
- 401 14 M. Blanco, M. Alcalá, J. M. Gonzalez, E. Torras, A Process Analytical Technology
402 Approach Based on Near Infrared Spectroscopy: Tablet Hardness, Content Uniformity,
403 and Dissolution Test Measurements of Intact Tablets, *J. Pharm. Sci.*, 2006, **95**(10),
404 2137-2144.

- 405 15 M. Donosso, E. S. Ghaly, Prediction of Drug Dissolution from Tablets Using Near-
406 Infrared Diffuse Reflectance Spectroscopy as a Nondestructive Method, *Pharm. Dev.*
407 *Technol.*, 2004, **9**(3), 247-263.
- 408 16 M. P. Freitas, A. Sabadin, L. M. Silva, F. M. Giannotti, D. A. do Couto, E. Tonhi, R. S.
409 Medeiros, G. L. Coco, V. F. T. Russo, J. A. Martins, Prediction of drug dissolution
410 profiles from tablets using NIR diffuse reflectance spectroscopy: A rapid and
411 nondestructive method, *J. Pharm. Biomed. Anal.*, 2005, **39**(1-2), 17-21.
- 412 17 C. Gendre, M. Boiret, M. Genty, P. Chaminade, L. M. Pean, Real-time predictions of
413 drug release and end point detection of a coating operation by in-line near infrared
414 measurements, *Int. J. Pharm.*, 2011, **421**(2), 237-243.
- 415 18 M. J. Waring, M. H. Rubinstein, J. R. Howard, Acoustic emission of pharmaceutical
416 materials: the effect of compression speed, ejection, lubrication and tablet weight, *Int. J.*
417 *Pharm.*, 1987, **40**(1-2), 15-22.
- 418 19 A. Hakanen, E. Laine, Acoustic Characterization of a Microcrystalline Cellulose Powder
419 During and After Its Compression, *Drug Dev. Ind. Pharm.*, 1995, **21**(13), 1573-1582.
- 420 20 J. Salonen, K. Salmi, A. Hakanen, E. Laine, K. Linsaari, Monitoring the acoustic activity
421 of a pharmaceutical powder during roller compaction, *Int. J. Pharm.*, 1997, **153**(2),
422 257-261.
- 423 21 T. Yoshida, T. Tanino, Y. Sumi, F. Nogami, Coating and polishing methods, and the
424 surface treatment apparatus to do by the methods, *JP Pat.*, Tokkai 2001-252548
425 (P2001-252548A), 2001.

- 426 22 P. J. Tilly, S. Porada, C. B. Scruby, S. Lidington, Monitoring of mixing processes using
427 acoustic emission, in *Fluid Mixing III*, eds. N. Harnby, H. Benkreira, K. J. Carpenter, R.
428 Mann, Institution of Chemical Engineers, Rugby, 1988.
- 429 23 M. F. Leach, G. A. Rubin, Size Analysis of Particles of Irregular Shape from their
430 Acoustic Emissions, *Powder. Technol.*, 1978, **21**(2), 263-267.
- 431 24 M. F. Leach, G. A. Rubin, J. C. Williams, Particle Size Distribution Characterization
432 from Acoustic Emissions, *Powder. Technol.*, 1978, **19**(2), 157-167.
- 433 25 M. Whitaker, G. R. Baker, J. Westrup, P. A. Goulding, D. R. Rudd, R. M. Belchamber,
434 M. P. Collins, Application of acoustic emission to the monitoring and end point
435 determination of a high shear granulation process, *Int. J. Pharm.*, 2000, **205**(1-2), 79-91.
- 436 26 L. Briens, D. Daniher, A. Tallevi, Monitoring high-shear granulation using sound and
437 vibration measurements, *Int. J. Pharm.*, 2007, **331**(1), 54-60.
- 438 27 H. E. Bass, A. J. Campanella, J. P. Chambers, R. B. Lindsay, Sound absorption,
439 AccessScience@McGraw-Hill, <http://www.accessscience.com.proxy2.lib.uwo.ca:2048>,
440 (Retrieved May 2008), DOI: 10.1036/1097-8542.637300.
- 441 28 D. Daniher, L. Briens, A. Tallevi, End-point detection in high-shear granulation using
442 sound and vibration signal analysis, *Powder Technol.*, 2008, **181**(2), 130-136.
- 443 29 L. D. Martin, J. V. Briongos, J. M. Aragon, M. C. Palancar, Can low frequency
444 accelerometry replace pressure measurements for monitoring gas-solid fluidized beds?,
445 *Chem. Eng. Sci.*, 2010, **65**(13), 4055-4064.

- 446 30 M. Halstensen, K. Esbensen, New developments in acoustic chemometric prediction of
447 particle size distribution - 'the problem is the solution', *J. Chemom.*, 2000, **14**(5-6),
448 463-481.
- 449 31 E. M. Hansuld, L. Briens, J. A. B. McCann, A. Sayani, Audible acoustics in high-shear
450 wet granulation: Application of frequency filtering, *Int. J. Pharm.*, 2009, **378**(1-2),
451 37-44.
- 452 32 Y. Li, J. R. Grace, R. B. Gopaluni, H. Bi, C. J. Lim, N. Ellis, Characterization of
453 gas-solid fluidization: A comparative study of acoustic and pressure signals, *Powder*
454 *Technol.*, 2011, **214**(2), 200-210.
- 455 33 K. H. Esbensen, P. Geladi, Principles of Proper Validation: use and abuse of re-sampling
456 for validation, *J. Chemom.*, 2010, **24**(3-4), 168-187.
- 457 34 F. N. Ihunegbo, C. Ratnayake, M. Halstensen, Acoustic chemometrics for on-line
458 monitoring and end-point determination of fluidised bed drying, *Powder Technol.*, 2013,
459 **247**, 69-75.
- 460 35 Sound & Vibration Technologies - about the sensor and sound -, Onosokki technical
461 report, http://www.onosokki.co.jp/HP-WK/c_support/newreport/sound/soundsensor.pdf,
462 (accessed December 2013).
- 463 36 Y. Hayashi, T. Sato, M. Otsuka, Real-time monitoring of the drying of
464 extruded-granules in a fluidized bed using near infrared spectroscopy and kinetic
465 evaluation of the drying process, *J. Near. Infrared. Spec.*, 2013, **21**(4), 107-115.
466
467

468

469 Figure Captions

470 Figure 1. Fluid-bed drying equipment for audible acoustic emission analysis.

471

472 Figure 2. Waveform of audible acoustic sound during the drying process of extruded
473 granules in the fluid-bed dryer.

474

475 Figure 3. **Change of (a) raw spectra, and (b) normalized spectra of AAE frequency**
476 **spectra during the drying process of extruded granules in the fluid-bed dryer.**

477

478 Figure 4. **Relationship between predicted and measured moisture contents of granules**
479 **based on (a) group 1, (b) group 7 of the PLS model, and (c) external validation result of**
480 **semi-external group 1-3 and external group 8 data using group 7, PLS model.**481 **External frequency spectral data under G1, G2, and G3 conditions were evaluated**
482 **using G1 and G7, PLS models.**483 **◇: G1 semi-external data, △: G2 semi-external data, and ▽: G3 data, ○: G8**
484 **external data.**

485

486 Figure 5. Loading vectors for group 7 of the PLS model based on normalized frequency
487 spectra of audible acoustic sound during the drying process of extruded granules in the
488 fluid-bed dryer.

489

490 Figure 6. Score plot of group 7, PLS model, based on normalized frequency spectra of
491 audible acoustic sound during the drying process of extruded granules in the fluid-bed dryer.

492

493 Figure 7. Regression vector for group 7, PLS model, based on normalized frequency
494 spectra of audible acoustic sound during the drying process of extruded granules in the
495 fluid-bed dryer.

496 Solid line is regression vector and gray line is frequency spectra of group 7.

497

498 Figure 8. External validation result of semi-external group 1-3, and external group 8 data
499 using groups 1 and 7, PLS model.

500 Closed circle is measured moisture under G1, G2, and G3 conditions, dashed line is
501 predicted by individual best-fitted PLS model, and solid line is predicted based on G7 PLS
502 model.

503

504 Table 1. Chemometric parameters for PLS calibration models based on audible acoustic
505 sound during the drying process to predict moisture content.

506 N, number of experiments; LV, latent variables; R^2 , coefficient of determination; PRESS,
507 predicted residual error sum of squares; RMSEC, root mean square error for calibration;
508 RMSEP, root mean square error for prediction; RMSECV, root mean square error for
509 cross-validation; group 1: standard conditions (42°C), group 2: including noise (vacuum
510 cleaner, Japanese pop music), group 3: low-thermal air (27°C), group 4: groups 1 + 2,
511 group 5: groups 1 + 3, group 6: groups 2 + 3, groups 7: groups 1 + 2 + 3.

512

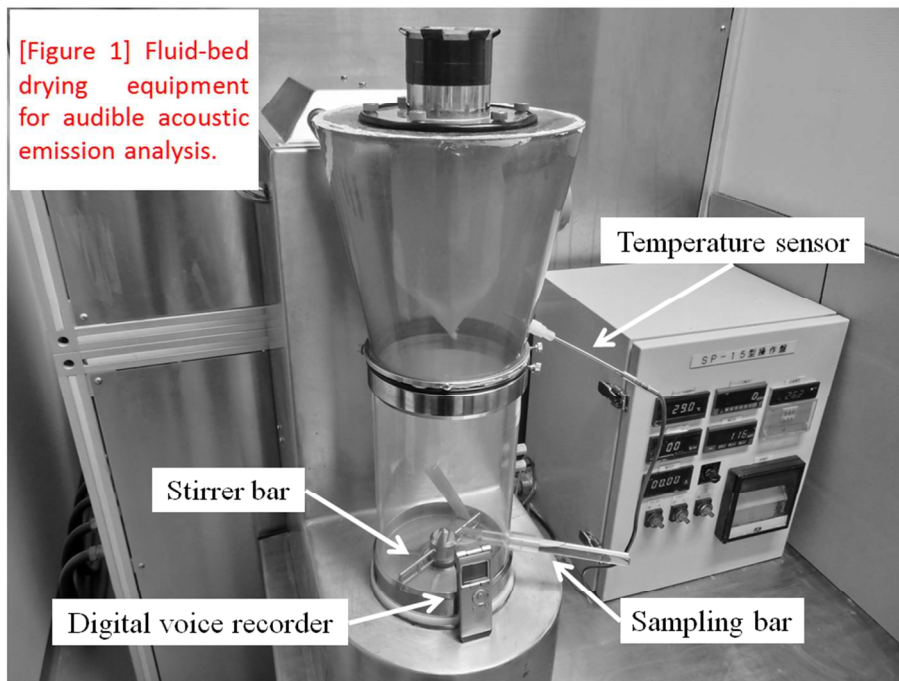
513 Table 2. Validation result of semi-external group 1-3 and external group 8 data using G1
514 or G7 PLS models.

515 **, best-fitted, *, second best-fitted, and frequency spectra of the external granular samples
516 obtained under G1, G2, and G3 conditions were evaluated using G1, G2, G3, and G7, PLS
517 models.

518

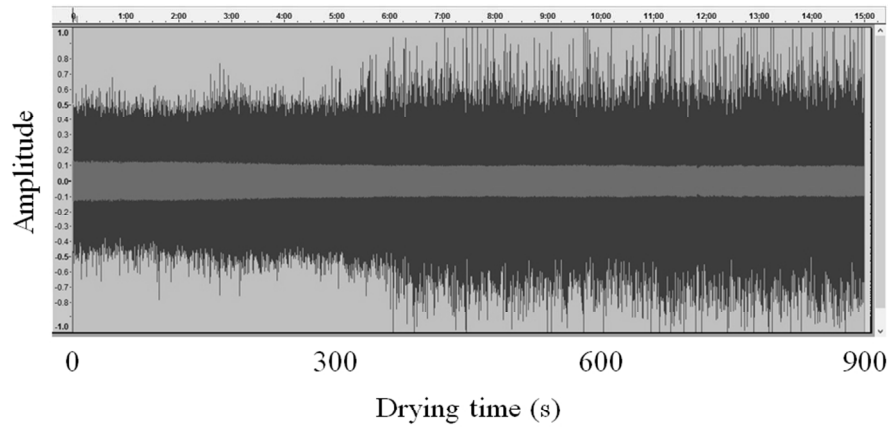
519

520



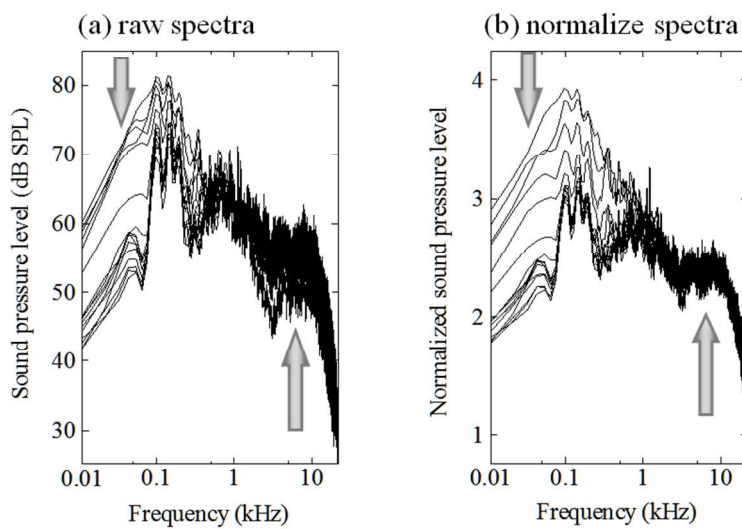
375x291mm (72 x 72 DPI)

[Figure 2] Waveform of audible acoustic sound during the drying process of extruded granules in the fluid-bed dryer.



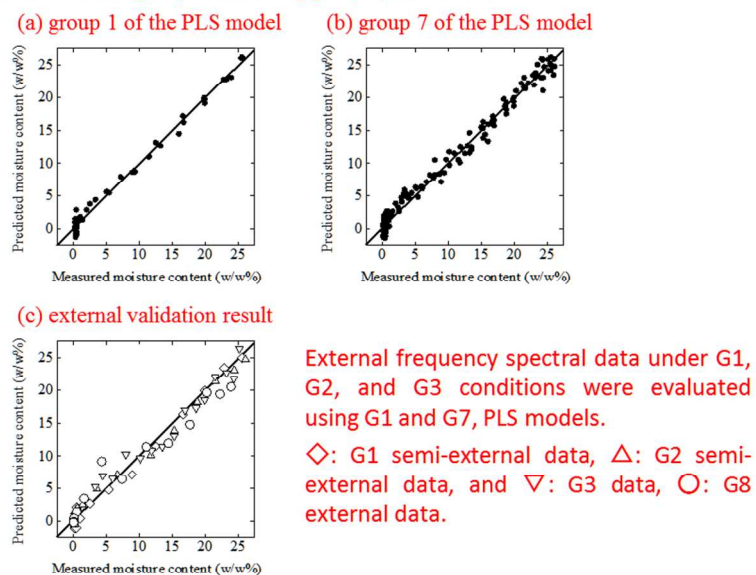
375x291mm (72 x 72 DPI)

[Figure 3] Change of (a) raw spectra, and (b) normalized spectra of AAE frequency spectra during the drying process of extruded granules in the fluid-bed dryer.



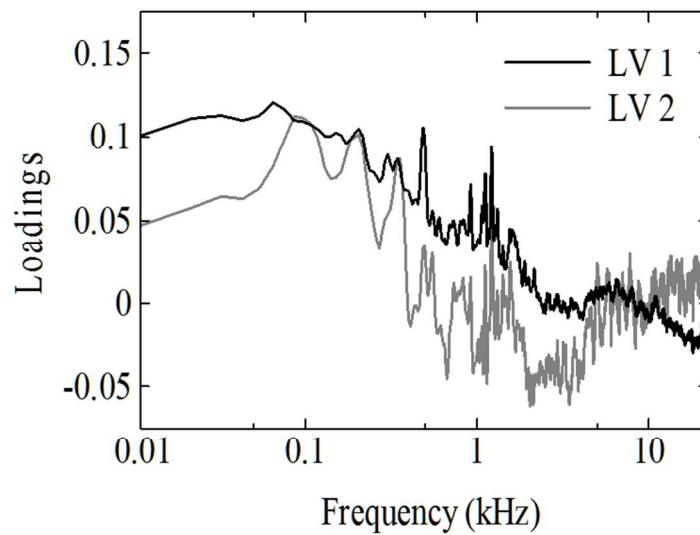
375x291mm (72 x 72 DPI)

[Figure 4] Relationship between predicted and measured moisture contents of granules based on (a) group 1, (b) group 7 of the PLS model, and (c) external validation result of semi-external group 1-3 and external group 8 data using group 7, PLS model.



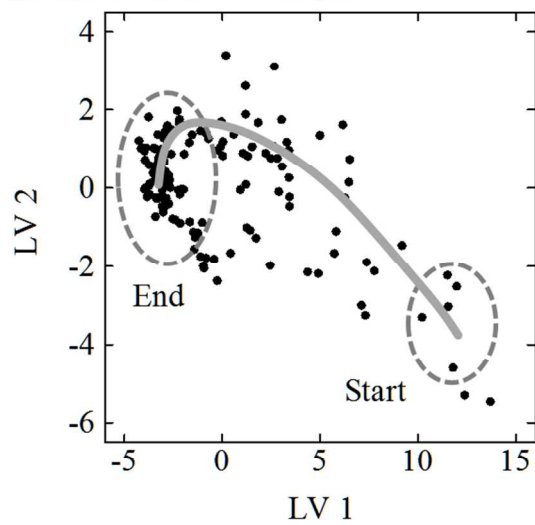
375x291mm (72 x 72 DPI)

[Figure 5] Loading vectors for group 7 of the PLS model based on normalized frequency spectra of audible acoustic sound during the drying process of extruded granules in the fluid-bed dryer.



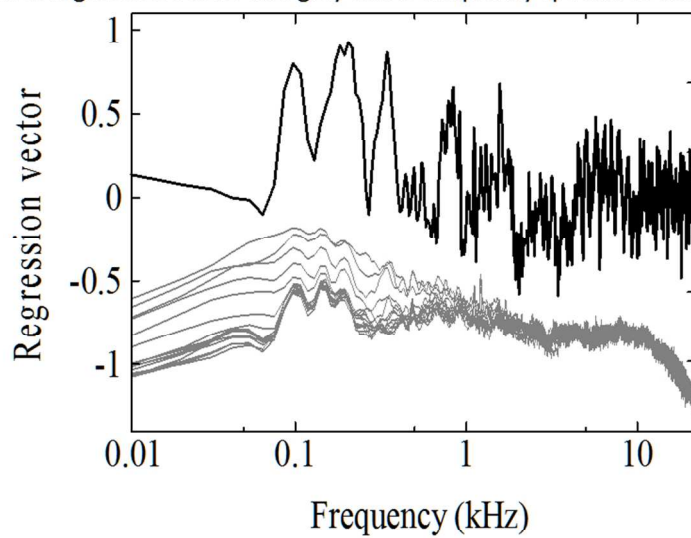
375x291mm (72 x 72 DPI)

[Figure 6] Score plot of group 7, PLS model, based on normalized frequency spectra of audible acoustic sound during the drying process of extruded granules in the fluid-bed dryer.



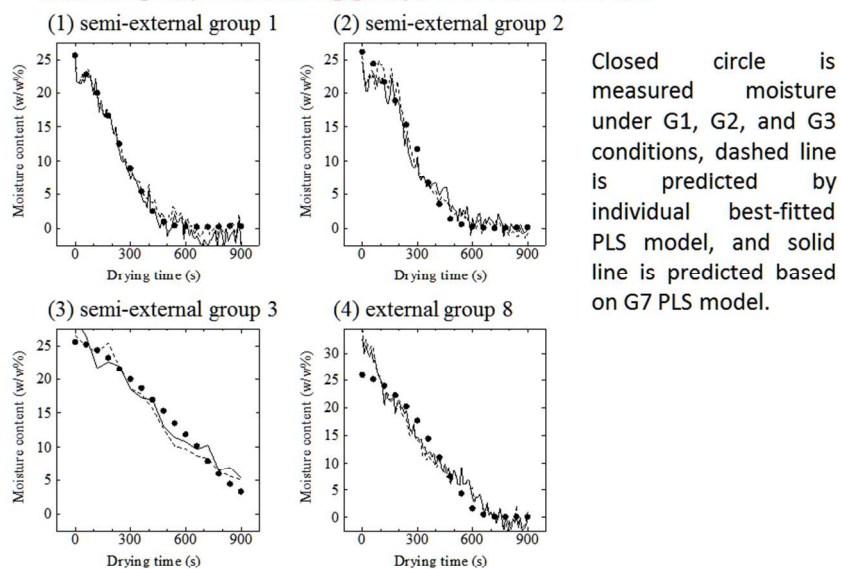
375x291mm (72 x 72 DPI)

[Figure 7] Regression vector for group 7, PLS model, based on normalized frequency spectra of audible acoustic sound during the drying process of extruded granules in the fluid-bed dryer. Solid line is regression vector and gray line is frequency spectra of the group 7.



375x291mm (72 x 72 DPI)

[Figure 8] External validation result of semi-external group 1-3, and external group 8 data using groups 1 and 7, PLS model.



375x291mm (72 x 72 DPI)

[Table 1] Chemometric parameters for PLS calibration models based on audible acoustic sound during the drying process to predict moisture content.

	N	LV	R ²	Slope	Intersept	PRESS	RMSEC	RMSEP	RMSECV
Group 1	3	4	0.992	0.992	0.0595	31.5	0.856	0.810	2.18
Group 2	3	4	0.992	0.992	0.0799	39.0	0.952	0.901	2.43
Group 3	3	4	0.992	0.992	0.116	18.7	0.692	0.651	1.79
Group 4	6	5	0.991	0.991	0.0784	80.4	0.945	0.915	2.21
Group 5	6	5	0.989	0.989	0.125	87.5	1.00	0.970	2.11
Group 6	6	5	0.987	0.987	0.158	101	1.08	1.05	2.23
Group 7	9	5	0.984	0.984	0.168	198	1.22	1.19	2.19

N, number of experiments; LV, latent variables; R², coefficient of determination; PRESS, predicted residual error sum of squares; RMSEC, root mean square error for calibration; RMSEP, root mean square error for prediction; RMSECV, root mean square error for cross-validation; group 1: standard conditions (42°C), group 2: including noise (Japanese pop music, vacuum cleaner, tableting machine), group 3: low temperature air (27°C), group 4: groups 1 + 2, group 5: groups 1 + 3, group 6: groups 2 + 3, group 7: groups 1 + 2 + 3.

254x190mm (96 x 96 DPI)

[Table 2] Validation result of semi-external group 1-3 and external group 8 data using G1 or G7 PLS models.

Batch	PLS model	R ²	Slope	Intersept	
Semi-external group 1	Group 1	0.991	0.985	0.479	**
	Group 2	0.980	1.210	0.142	
	Group 3	0.913	0.685	4.04	
	Group 7	0.985	1.03	-0.906	*
Semi-external group 2	Group 1	0.929	0.768	3.50	
	Group 2	0.992	0.987	0.117	*
	Group 3	0.848	0.593	6.50	
	Group 7	0.994	0.920	0.630	**
Semi-external group 3	Group 1	0.827	0.844	-0.845	
	Group 2	0.931	0.989	-0.129	
	Group 3	0.958	0.992	-0.273	**
	Group 7	0.938	0.940	0.988	*
External group 8	Group 1	0.892	0.983	0.800	
	Group 2	0.944	1.12	0.345	**
	Group 3	0.820	0.673	4.85	
	Group 7	0.928	0.988	0.396	*

** , best-fitted, * , second-best-fitted, and frequency spectra of the semi-external and external granular samples obtained under G1, G2, and G3 conditions were evaluated using G1, G2, G3, and G7, PLS models.

254x190mm (96 x 96 DPI)